Covariance-Based Direction-of-Arrival Estimation With Real Structures

Tadeu N. Ferreira, *Student Member, IEEE*, Sergio L. Netto, *Senior Member, IEEE*, and Paulo S. R. Diniz, *Fellow, IEEE*

***Abstract*—Parametric methods for direction-of-arrival (DoA) estimation have become very popular due to their low computational complexity and good accuracy. Among parametric DoA algorithms, ESPRIT is one of the most widely used, since it presents low computational complexity in comparison to other parametric methods. Covariance-based DoA (CB-DoA) estimation algorithm provides an even lower complexity alternative to ESPRIT, while imposing the same constraints on the geometry of the receiving array. This letter presents a new algorithm, based on the CB-DoA approach, comprising only real operations. The constraints on the algorithm are the same imposed to the unitary ESPRIT algorithm, allowing a reduction of about 67% on the required computational effort, for equivalent error measure.**

***Index Terms*—Antenna arrays, direction-of-arrival estimation, parameter estimation.**

I. Introduction

ESTIMATING the direction-of-arrival (DoA) of impinging waves for antenna-array receivers is a very useful tool for spatially separating sources in multiuser communication systems. Some DoA standard techniques, such as ESPRIT [1] and matrix-pencil (MP) methods [2], are based on parametric estimation techniques, which present lower computational complexity than previous nonparametric methods. MP methods are simpler than the ESPRIT method, at the cost of a more restricted constraint on the geometry of the receiving antenna array. Recently, a covariance-based DoA (CB-DoA) estimation algorithm [3], [4] was fully presented combining the ESPRIT-like translational invariance constraint and MSE performance with computational complexity advantages over MP methods.

This letter simplifies even further the CB-DoA algorithm, by imposing an additional geometrical constraint on the receiving antenna array, similar to the one employed by the unitary ESPRIT [5]. The proposed algorithm, although related, presents less restrictive constraints than the MP-based algorithm presented in [6]. Section II presents the formulation for the DoA problem with the additional constraints on the geometry of the receiving array. Section III describes the proposed real CB-DoA algorithm. Section IV compares the computational effort required by unitary ESPRIT and the proposed algorithm. Section V presents some computer simulations for both unitary ESPRIT and real CB-DoA, whereas Section VI summarizes the main conclusions of this work.

Manuscript received August 07, 2008; revised August 31, 2008. The associate editor coordinating the review of this manuscript and approving it for publication was Prof. Kainam Thomas Wong.

The authors are with the Electrical Engineering Program, Federal University of Rio de Janeiro, Rio de Janeiro, Brazil (e-mail: tadeu.n.ferreira@gmail.com; sergioln@lps.ufrj.br; diniz@lps.ufrj.br).

Color versions of one or more of the figures in this paper are available online at http://ieeexplore.ieee.org.

Digital Object Identifier 10.1109/LSP.2008.2007622

II. Basic Framework

In this section, the DoA system model is presented, focusing on the centro-Hermitian constraints, as well as TLS solution to the original complex-valued problem, as presented in [1] and [3].

A. General Structures

Consider a multiple-input multiple-output (MIMO) environment with M transmitting and $2N$ receiving antennas, with $N > M$. Each channel is corrupted by an additive white Gaussian noise (AWGN). The receiving antennas are grouped in pairs (doublets). In each doublet, there is a constant displacement Δ between the antennas, providing a translational invariance in the geometry of the array. If one divides the antennas of the receiving array in two sub-arrays, where each doublet is split between the sub-arrays, the received signal $x_{l,i}(t)$, for the ith antenna in the lth sub-array, is represented by

$$x_{l,i}(t) = \sum_{m=0}^{M-1} s_m(t) a_{l,i}(\theta_m) + n_{l,i}(t) \tag{1}$$

for $l = 0, 1$ and $i = 0, 1, \ldots, (N-1)$, where $a_{l,i}(\theta_m)$ refers to the gain of the (l,i)th receiving antenna for the impinging angle θ_m of the signal $s_m(t)$ transmitted by the mth antenna, and $n_{l,i}(t)$ denotes the associated noise component. The same receiving antenna may belong to both sub-arrays, since each antenna may belong to two different doublets. Considering uniform time-sampling, the discrete receiving snapshots may be represented as

$$\begin{bmatrix} \mathbf{J}_0 \\ \mathbf{J}_1 \end{bmatrix} \mathbf{x}(k) = \begin{bmatrix} \mathbf{x}_0(k) \\ \mathbf{x}_1(k) \end{bmatrix} = \begin{bmatrix} \mathbf{A}_0 \\ \mathbf{A}_1 \end{bmatrix} \mathbf{s}(k) + \begin{bmatrix} \mathbf{n}_0(k) \\ \mathbf{n}_1(k) \end{bmatrix} \tag{2}$$

where $\mathbf{J}_0 = [\mathbf{I}_N \quad \mathbf{0}_N]$ and $\mathbf{J}_1 = [\mathbf{0}_N \quad \mathbf{I}_N]$ are selection matrices, used for separating the antennas into sub-arrays, $\mathbf{x}_l(k) = [x_{l,0}(k) \quad x_{l,1}(k) \quad \ldots \quad x_{l,(N-1)}(k)]^T$ represents the received snapshot in the lth sub-array, and $\mathbf{n}_l(k) = [n_{l,0}(k) \quad n_{l,1}(k) \quad \ldots \quad n_{l,(N-1)}(k)]^T$ represents the noise vector. The receiving sub-array matrix $\mathbf{A}_l$, which represents the directional gains for the lth sub-array, is defined by $[\mathbf{A}_l]_{i,j} = a_{l,i}(\theta_j)$, with $i = 0, 1, \ldots, (N-1)$, and $j = 0, 1, \ldots, (M-1)$. Besides that, $\mathbf{s}(k) = [s_0(k) \quad s_1(k) \quad \ldots \quad s_{(M-1)}(k)]^T$ is the transmitted data structure. The larger structure $\mathbf{A} = [\mathbf{A}_0^T \quad \mathbf{A}_1^T]^T$ comprising the gains of the overall receiving array is known as

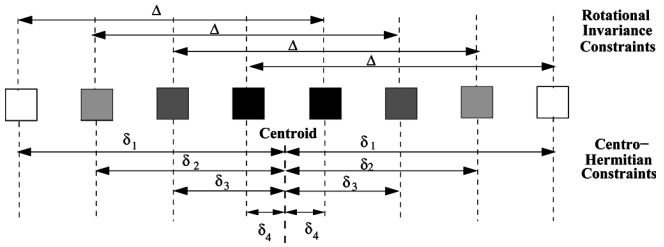

Fig. 1. Receiving array with the constraints of both rotational invariance, as well as the new centro-Hermitian constraints. Antennas with the same pattern should have the same receiving characteristics.

the array manifold. Due to the constant displacement Δ of the receiving doublets, there is a unitary diagonal matrix $\mathbf{\Phi}$ such that

$$\mathbf{A}_1 = \mathbf{A}_0\mathbf{\Phi}. \tag{3}$$

Each diagonal element ϕ_i of $\mathbf{\Phi}$ is related to the DoA by the expression [5]

$$\phi_i = \exp\left(\frac{-j2\pi f\Delta\sin(\theta_i)}{c}\right) \tag{4}$$

where c represents the speed of light and f is the frequency for transmission.

In order to perform only real operations, matrix $\mathbf{A}$ must be also centro-Hermitian, that is, [5]

$$\mathbf{\Pi}_{2N}\mathbf{A}^*\mathbf{\Pi}_M = \mathbf{A} \tag{5}$$

where $\mathbf{\Pi}_i$ refers to an $i \times i$-permutation matrix with ones in its main antidiagonal and zeros outside, and the superscript asterisk represents the conjugate operation. Geometrically, an array is considered centro-Hermitian if its elements are symmetric with respect to the centroid, as represented in Fig. 1, and the receiving characteristics of symmetrically located antenna pairs are equivalent [5].

For a given $a \times a$ matrix $\mathbf{M}$, where a is even, consider the transformation ψ and rotation matrix $\mathbf{Q}_a$ such that

$$\psi(\mathbf{M}) = \mathbf{Q}_a^H\mathbf{M}\mathbf{Q}_a \tag{6}$$

$$\mathbf{Q}_a = \frac{1}{\sqrt{2}}\begin{bmatrix}\mathbf{I}_{a/2} & j\mathbf{I}_{a/2}\\ \mathbf{\Pi}_{a/2} & -j\mathbf{\Pi}_{a/2}\end{bmatrix}. \tag{7}$$

For odd values of a, some changes are needed in the structure of $\mathbf{Q}_a$, without affecting the following results. It is shown in [5] that the ψ operation transforms a centro-Hermitian matrix into a matrix containing only real elements. Moreover, if $\mathbf{U}_\mathbf{Y}$ denotes the matrix containing the eigenvectors of $\mathbf{Y}$, then one has that

$$\mathbf{U}_\mathbf{M} = \mathbf{Q}_a\mathbf{U}_{\psi(\mathbf{M})}. \tag{8}$$

For any $a \times a$ matrix $\mathbf{M}$, the extended matrix

$$\mathcal{E}(\mathbf{M}) = [\,\mathbf{M} \quad \mathbf{\Pi}_a\mathbf{M}^*\mathbf{\Pi}_a\,] \tag{9}$$

is centro-Hermitian. Therefore, the composite transformation $\mathcal{T}(\mathbf{M}) = \psi(\mathcal{E}(\mathbf{M}))$ yields a real matrix.

B. TLS Solution to the Original DoA Problem

Consider matrix $\mathbf{X}$ comprising K snapshots of $\mathbf{x}(k)$ in its columns. Defining $\mathbf{Z}$ the forward-backward (FB) structure for the received snapshots, $\mathbf{Z} = [\mathbf{X}\ \mathbf{\Pi}_{2N}\mathbf{X}^*]$, then it can be shown that the FB correlation matrix $\mathbf{R} = \mathcal{T}(\mathbf{X})\mathcal{T}^H(\mathbf{X})$ may be expressed as

$$\mathbf{R} = \mathbf{Q}_{2N}^H\mathbf{Z}\mathbf{Z}^H\mathbf{Q}_{2N} = \psi(\mathbf{Z}\mathbf{Z}^H) \tag{10}$$

such that, from the property stated in (8)

$$\mathbf{U}_\mathbf{R} = \mathbf{Q}_{2N}\mathbf{U}_{\mathbf{Z}\mathbf{Z}^H}. \tag{11}$$

By partitioning $\mathbf{U}_{\mathbf{Z}\mathbf{Z}^H}$ as

$$\mathbf{U}_{\mathbf{Z}\mathbf{Z}^H} = \begin{bmatrix}\mathbf{C}_0\\ \mathbf{C}_1\end{bmatrix} \tag{12}$$

the new geometric constraint on the receiving antennas leads to an invariance relation $\mathbf{C}_0\mathbf{\Psi} = \mathbf{C}_1$ [5], whose total least-squares (TLS) solution $\mathbf{\Psi}_{\mathrm{TLS}}$ may be determined by an eigendecomposition operation [7]

$$\begin{aligned}\mathbf{C}_{\mathrm{TLS}} &= \begin{bmatrix}\mathbf{C}_0^H\\ \mathbf{C}_1^H\end{bmatrix}[\,\mathbf{C}_0 \quad \mathbf{C}_1\,]\\ &= \mathbf{U}_{\mathbf{C}_{\mathrm{TLS}}}\mathbf{\Sigma}^2\mathbf{U}_{\mathbf{C}_{\mathrm{TLS}}}^H\\ &= \begin{bmatrix}\mathbf{V}_{00} & \mathbf{V}_{01}\\ \mathbf{V}_{10} & \mathbf{V}_{11}\end{bmatrix}\begin{bmatrix}\mathbf{\Sigma}_1^2 & \mathbf{0}\\ \mathbf{0} & \mathbf{\Sigma}_2^2\end{bmatrix}\begin{bmatrix}\mathbf{V}_{00}^H & \mathbf{V}_{10}^H\\ \mathbf{V}_{01}^H & \mathbf{V}_{11}^H\end{bmatrix}\end{aligned} \tag{13}$$

followed by the matrix multiplication

$$\mathbf{\Psi}_{\mathrm{TLS}} = -\mathbf{V}_{01}\mathbf{V}_{11}^{-1}. \tag{14}$$

C. Equivalent TLS Problem

From the definitions of the transformations $\mathcal{T}$ and ψ in Section II-A

$$\mathcal{T}(\mathbf{C}_0) = \mathbf{Q}_N^H[\,\mathbf{C}_0 \quad \mathbf{C}_1\,]\begin{bmatrix}\mathbf{I}_K & \mathbf{0}_K\\ \mathbf{0}_K & \mathbf{\Pi}_K\end{bmatrix}\mathbf{Q}_{2K}. \tag{15}$$

Defining $\mathbf{P} = \mathcal{T}^H(\mathbf{C}_0)\mathcal{T}(\mathbf{C}_0)$, then one has that

$$\mathbf{P} = \mathbf{Q}_{2K}^H\begin{bmatrix}\mathbf{I}_K & \mathbf{0}_K\\ \mathbf{0}_K & \mathbf{\Pi}_K\end{bmatrix}\mathbf{C}_{\mathrm{TLS}}\begin{bmatrix}\mathbf{I}_K & \mathbf{0}_K\\ \mathbf{0}_K & \mathbf{\Pi}_K\end{bmatrix}\mathbf{Q}_{2K}. \tag{16}$$

Hence, by partitioning $\mathbf{U}_\mathbf{P}$ as

$$\mathbf{U}_\mathbf{P} = \begin{bmatrix}\mathbf{W}_{00} & \mathbf{W}_{01}\\ \mathbf{W}_{10} & \mathbf{W}_{11}\end{bmatrix} \tag{17}$$

an alternative TLS solution may be determined as [7]

$$\mathbf{\Upsilon}_{\mathrm{TLS}} = -\mathbf{W}_{01}\mathbf{W}_{11}^{-1} \tag{18}$$

which is related to the original TLS solution by

$$\mathbf{\Psi}_{\mathrm{TLS}} = -(\mathbf{\Upsilon}_{\mathrm{TLS}} - j\mathbf{I}_N)(\mathbf{\Upsilon}_{\mathrm{TLS}} + j\mathbf{I}_N)^{-1}. \tag{19}$$

TABLE I
SHORT DESCRIPTIONS OF UNITARY ESPRIT AND REAL CB-DOA ALGORITHMS

Unitary ESPRIT	Real CB-DoA
$\mathbf{\Xi} = \mathbf{\Pi}_N \mathbf{J}_0 \mathbf{\Pi}_{2N}$	$\mathbf{\Xi} = \mathbf{\Pi}_N \mathbf{J}_0 \mathbf{\Pi}_{2N}$
$\mathbf{K}_0 = \mathbf{Q}_N^H(\mathbf{J}_0 + \mathbf{\Xi})\mathbf{Q}_{2K}$	$\mathcal{E}_Q(\mathbf{X}) = \mathcal{E}(\mathbf{X})\mathbf{Q}_{2K}$
$\mathbf{K}_1 = \mathbf{Q}_N^H(\mathbf{J}_0 - \mathbf{\Xi})\mathbf{Q}_{2K}$	$\mathcal{T}_0(\mathbf{X}) = \mathbf{Q}_N^H(\mathbf{J}_0 + \mathbf{\Xi})\mathcal{E}_Q(\mathbf{X})$
$\mathcal{T}(\mathbf{X}) = \mathbf{Q}_{2N}^H \mathcal{E}(\mathbf{X})\mathbf{Q}_{2K}$	$\mathcal{T}_1(\mathbf{X}) = \mathbf{Q}_N^H j(\mathbf{J}_0 - \mathbf{\Xi})\mathcal{E}_Q(\mathbf{X})$
$\mathbf{R} = \mathcal{T}(\mathbf{X})\mathcal{T}^H(\mathbf{X})$	$\mathbf{R}_{00} = \mathcal{T}_0(\mathbf{X})\mathcal{T}_0^H(\mathbf{X})$
$[\mathbf{U}_{\mathbf{R}_s}, \mathbf{\Sigma}^2_{\mathbf{R}_s}] = \text{EVD}(\mathbf{R})$	$[\mathbf{U}_{00,s}, \mathbf{\Sigma}^2_{00,s}] = \text{EVD}(\mathbf{R}_{00})$
$\mathbf{E}_x = \mathbf{K}_0\mathbf{U}_{\mathbf{R}_s}$, $\mathbf{E}_y = \mathbf{K}_1\mathbf{U}_{\mathbf{R}_s}$	
$\mathbf{E}_{\text{TLS}} = \begin{bmatrix}\mathbf{E}_x & \mathbf{E}_y\end{bmatrix}^H \begin{bmatrix}\mathbf{E}_x & \mathbf{E}_y\end{bmatrix}$	
$[\mathbf{U}_{\mathbf{E}_{\text{TLS}}}, \mathbf{\Lambda}] = \text{EVD}(\mathbf{E}_{\text{TLS}})$	$\mathbf{F} = \mathbf{\Sigma}_{00,s}^{-1}\mathbf{U}_{00,s}^H$
$\begin{bmatrix}\mathbf{E}_{00} & \mathbf{E}_{01}\\ \mathbf{E}_{10} & \mathbf{E}_{11}\end{bmatrix} = \mathbf{U}_{\mathbf{E}_{\text{TLS}}}$	$\mathbf{R}_{10} = \mathcal{T}_1(\mathbf{X})\mathcal{T}_0(\mathbf{X})^H - \hat{\sigma}^2\mathbf{I}$
$\mathbf{\Upsilon} = -\mathbf{E}_{01}\mathbf{E}_{11}^{-1}$	$\mathbf{R}_{\mathbf{F}} = \mathbf{F}\mathbf{R}_{10}\mathbf{F}^H$
$[\mathbf{U}_{\mathbf{\Upsilon}}, \mathbf{\Omega}] = \text{EVD}(\mathbf{\Upsilon})$	$[\mathbf{H}\mathbf{U}_{\mathbf{\Upsilon}}, \mathbf{\Omega}] = \text{EVD}(\mathbf{R}_{\mathbf{F}})$
$\hat{\theta}_i = 2\arctan(\omega_i)$	$\hat{\theta}_i = 2\arctan(\omega_i)$

III. REAL CB-DOA ALGORITHM

Both (14) and (18) involve complex operations. In this section, an equivalent and computationally simpler solution to these equations is presented based only on real operations.

A. TLS Solution With Real Operations

Let $\mathbf{U}_{\mathbf{R}_s}$ comprise the eigenvectors of $\mathbf{R}$ associated to the signal subspace. From the definitions of $\mathcal{T}$, $\mathbf{Q}_{2K}$, $\mathbf{J}_0$, and $\mathbf{J}_1$, then (15) may be rewritten as

$$\mathcal{T}(\mathbf{C}_0) = \frac{1}{\sqrt{2}}\mathbf{Q}_N^H \begin{bmatrix}\mathbf{J}_0\mathbf{Q}_{2N}\mathbf{U}_{\mathbf{R}_s} & \mathbf{J}_1\mathbf{Q}_{2N}\mathbf{U}_{\mathbf{R}_s}\end{bmatrix} \begin{bmatrix}\mathbf{I}_K & j\mathbf{I}_K\\ \mathbf{I}_K & -j\mathbf{I}_K\end{bmatrix}. \quad (20)$$

By defining the new selection matrices

$$\mathbf{K}_0 = \mathbf{Q}_N^H(\mathbf{J}_0 + \mathbf{\Pi}_N\mathbf{J}_0\mathbf{\Pi}_{2N})\mathbf{Q}_{2N} \quad (21)$$

$$\mathbf{K}_1 = \mathbf{Q}_N^H j(\mathbf{J}_0 - \mathbf{\Pi}_N\mathbf{J}_0\mathbf{\Pi}_{2N})\mathbf{Q}_{2N} \quad (22)$$

then, since $\mathbf{J}_0 = \mathbf{\Pi}_N\mathbf{J}_1\mathbf{\Pi}_{2N}$, one has that

$$\mathcal{T}(\mathbf{C}_0) = \frac{1}{\sqrt{2}}\begin{bmatrix}\mathbf{K}_0\mathbf{U}_{\mathbf{R}_s} & \mathbf{K}_1\mathbf{U}_{\mathbf{R}_s}\end{bmatrix}. \quad (23)$$

From (20), the structure of $\mathcal{T}(\mathbf{C}_0)$ has an invariance equation property that may be expressed as

$$\mathbf{K}_0\mathbf{U}_{\mathbf{R}_s}\mathbf{\Upsilon} = \mathbf{K}_1\mathbf{U}_{\mathbf{R}_s} \quad (24)$$

which is the core of the unitary ESPRIT algorithm [5]. Performing an eigenvalue decomposition on $\mathbf{\Upsilon}$, such that $\mathbf{\Upsilon} = \mathbf{U}_{\mathbf{\Upsilon}}\mathbf{\Omega}\mathbf{U}_{\mathbf{\Upsilon}}^H$, the DoA estimation $\hat{\theta}_i = 2\arctan(\omega_i)$ results based on the diagonal elements ω_i of $\mathbf{\Omega}$.

B. Real Covariance-Based Approach

Consider the covariance matrix $\mathbf{R}$ of the output signal, as given in (10), and the received data matrix $\mathbf{Z}$, corrupted by noise, as presented in Section II-B. Using selection matrices $\mathbf{K}_0$ and $\mathbf{K}_1$, new covariance structures are defined as

$$\begin{aligned}\mathbf{R}_{00} &= \mathbf{K}_0(\mathbf{R} - \hat{\sigma}^2\mathbf{I})\mathbf{K}_0^H\\ &= \mathbf{K}_0\mathbf{Q}_{2N}^H(\mathbf{Z}\mathbf{Z}^H - \hat{\sigma}^2\mathbf{I})\mathbf{Q}_{2N}\mathbf{K}_0^H \quad (25)\\ \mathbf{R}_{10} &= \mathbf{K}_1(\mathbf{R} - \hat{\sigma}^2\mathbf{I})\mathbf{K}_0^H\\ &= \mathbf{K}_1\mathbf{Q}_{2N}^H(\mathbf{Z}\mathbf{Z}^H - \hat{\sigma}^2\mathbf{I})\mathbf{Q}_{2N}\mathbf{K}_0^H \quad (26)\end{aligned}$$

TABLE II
NUMBER OF MATRIX OPERATIONS REQUIRED BY UNITARY ESPRIT AND REAL CB-DOA

Operation	Unitary ESPRIT		Real CB-DoA	
	#	Flops [8]	#	Flops [8]
EVD	1	$25M^3$	1	$25M^3$
Hermitian EVD	2	$4N^2 + 4M^2$	1	M^2
Full Inverse	1	$(25/3)M^3$	–	–
Diag. Inverse	–	–	1	M
Multiplication	16	$4M^2N+4MN^2+M^3+18N^3+12N^2K+12NK^2$	12	$4N^2K+2M^2N+MN^2+10N^3+4NK^2$

where $\hat{\sigma}^2$ is the estimated noise power. Performing the eigendecomposition $\mathbf{R}_{00} = \mathbf{U}_{\mathbf{R}_{00}}\mathbf{\Sigma}^2_{00}\mathbf{U}^H_{\mathbf{R}_{00}}$, one can establish the signal subspace by grouping the largest eigenvalues of $\mathbf{\Sigma}^2_{00}$ into $\mathbf{\Sigma}^2_{00,s}$ and their associated eigenvectors into matrix $\mathbf{U}_{00,s}$. Then, one has

$$\mathbf{K}_0\mathbf{Q}_{2N}^H\mathbf{S} = \mathbf{U}_{00,s}\mathbf{\Sigma}_{00,s}\mathbf{H} \quad (27)$$

where $\mathbf{H}$ is a full-rank matrix, and $\mathbf{S} = [\mathbf{s}(0)\ \mathbf{s}(1)\ \ldots\ \mathbf{s}(K-1)]$ is the noiseless overall transmitted data matrix. From (24) and (27)

$$\mathbf{K}_1\mathbf{Q}_{2N}^H\mathbf{S} = \mathbf{K}_0\mathbf{Q}_{2N}^H\mathbf{S}\mathbf{\Upsilon} = \mathbf{U}_{00,s}\mathbf{\Sigma}_{00,s}\mathbf{H}\mathbf{\Upsilon}. \quad (28)$$

Defining the transformation $\mathbf{F} = \mathbf{\Sigma}_{00,s}^{-1}\mathbf{U}_{00,s}^H$, such that

$$\mathbf{F}\mathbf{K}_0\mathbf{Q}_{2N}^H\mathbf{S} = \mathbf{H} \quad (29)$$

and applying it onto $\mathbf{R}_{10}$, one gets

$$\begin{aligned}\mathbf{R}_{\mathbf{F}} &= \mathbf{F}\mathbf{R}_{10}\mathbf{F}^H\\ &= \mathbf{F}\mathbf{K}_1\mathbf{Q}_{2N}^H(\mathbf{Z}\mathbf{Z}^H - \hat{\sigma}^2\mathbf{I})\mathbf{Q}_{2N}\mathbf{K}_0^H\mathbf{F}^H\\ &= \mathbf{F}\mathbf{K}_1\mathbf{Q}_{2N}^H\mathbf{S}\mathbf{S}^H\mathbf{Q}_{2N}\mathbf{K}_0^H\mathbf{F}^H\\ &= \mathbf{F}\mathbf{K}_0\mathbf{Q}_{2N}^H(\mathbf{S}\mathbf{\Upsilon}\mathbf{S}^H)\mathbf{Q}_{2N}\mathbf{K}_0^H\mathbf{F}^H\\ &= \mathbf{H}\mathbf{\Upsilon}\mathbf{H}^H\\ &= \mathbf{H}\mathbf{U}_{\mathbf{\Upsilon}}\mathbf{\Omega}\mathbf{U}_{\mathbf{\Upsilon}}^H\mathbf{H}^H. \quad (30)\end{aligned}$$

Hence, matrix $\mathbf{\Omega}$ is determined by the eigendecomposition of matrix $\mathbf{R}_{\mathbf{F}}$, leading to the DoA estimation $\hat{\theta}_i = 2\arctan(\omega_i)$, as before.

IV. COMPUTATIONAL COMPLEXITY ANALYSIS

In this section, the proposed real CB-DoA and the unitary ESPRIT algorithms, summarized in Table I, are compared with respect to their computational complexity. Consider N as the number of elements in each subarray, M as the number of sources, $2N$ as the amount of sensors, and K as the amount of snapshots used. A more direct comparison between unitary ESPRIT and real CB-DoA is addressed by Table II, which includes the complexity effort associated to each matrix operation for both algorithms.

Since K represents the number of samples, it is, in general, much larger than the amount of antennas. Then, the term containing K^2 tends to dominate the complexity analysis. For large K, the computational requirement for the real CB-DoA becomes approximately 33% of the one required by unitary ESPRIT.

One may also make a comparison to MP methods. MP uses the first six operations as defined in Table I for ESPRIT, which are the most computationally complex ones, including the dominant term $12K^2$ present in the flop analysis. MP methods require one generalized EVD, much more complex than the traditional EVD. Therefore, real CB-DoA is less computationally complex than MP. In addition, MP requires the additional constraint that the receiving array must present uniformly spaced elements.

V. Simulations

Some experiments were included to compare the performance of real CB-DoA algorithm to the standard unitary ESPRIT algorithm. Signal from each source was randomly generated from a Gaussian distribution. Both the array manifold matrix and the DoA gain vector were randomly determined.

The performance assessment is based on the mean-square error (MSE) between the estimated $\hat{\theta}_i$ and actual θ_i arriving angles, that is, MSE $= 1/M \sum_i |\theta_i - \hat{\theta}_i|^2$, $0 \leq i \leq M-1$. The MSE value, measured by an ensemble average over 300 runs, was determined for distinct values of the signal-to-noise ratio (SNR) measured over 7500 snapshots, taken at the receiver input. The results are presented in Fig. 2. Simulations were performed using two transmitting sources and 12 receiving antennas. Afterwards, two more sources were added in the scenario. The receiving array geometry is constrained to present both translational invariance, as well as being centro-Hermitian, as described in Section II.

From Fig. 2, one may conclude that the measured MSEs are quite close for both algorithms for the whole simulated range of SNR. The MSE result is also comparable to the performance of original CB-DoA and ESPRIT algorithms [3]. For both scenarios, the amount of flops required by real CB-DoA is approximately 33% of the flops required by unitary ESPRIT. Simulations with different numbers of sources or receiving antennas also present similar MSE results and computational savings.

VI. Conclusions

This work proposed an alternative algorithm to covariance-based determination of direction-of-arrival (CB-DoA), whose computational complexity is further reduced by using strictly real operations, after imposing a central-symmetric constraint on the geometry of the receiving antenna array. Computational analysis and computer simulations show that the proposed real CB-DoA algorithm presents 67% less computing operations and equivalent MSE performance in comparison to unitary ESPRIT algorithm, an accelerated version of ESPRIT. Computational advantages are also observed over MP methods.

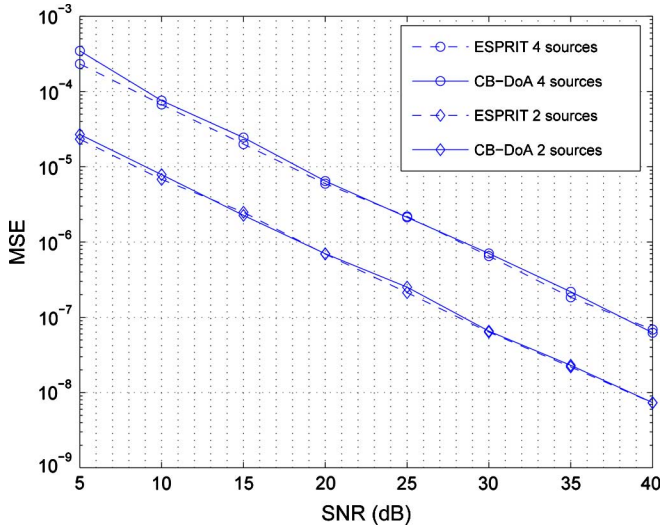

Fig. 2. MSE comparison for unitary ESPRIT and real CB-DoA algorithms, for two simulation scenarios: using two and four sources, respectively, and a receiving array of 12 antennas, in both scenarios.

References

[1] R. Roy and T. Kailath, "ESPRIT—estimation of parameters via rotational invariance techniques," *IEEE Trans. Acoust., Speech, Signal Process.*, vol. ASSP-37, no. 7, pp. 984–995, Jul. 1989.

[2] J. Razavilar, Y. Li, and K. J. R. Liu, "Spectral estimation based on structured low rank matrix pencil," in *Proc. 22nd. IEEE Int. Conf Acoustics, Speech and Signal Processing*, May 1996, vol. 5, pp. 2503–2506.

[3] T. N. Ferreira, S. L. Netto, and P. S. R. Diniz, "Low complexity covariance-based DoA estimation algorithm," in *Proc. 15th EURASIP Eur. Signal Processing Conf.*, Poznan, Poland, Sep. 2007, pp. 100–104.

[4] M. D. Zoltowski, "Solving the generalized eigenvalue problem with singular forms," *Proc. IEEE*, vol. 75, no. 11, pp. 1546–1548, Nov. 1987.

[5] M. Haardt and J. A. Nossek, "Unitary ESPRIT: How to obtain increased estimation accuracy with a reduced computational burden," *IEEE Trans. Acoust., Speech, Signal Process.*, vol. 43, no. 5, pp. 1232–1242, May 1995.

[6] N. Yilmazer, J. Koh, and T. K. Sarkar, "Utilization of a unitary transform for efficient computation in the matrix pencil method to find the direction of arrival," *IEEE Trans. Antennas Propag.*, vol. 54, no. 1, pp. 175–181, Jan. 2006.

[7] I. Markovsky and S. van Huffel, "Overview of total least-squares methods," *Signal Process.*, vol. 87, pp. 2283–2302, Oct. 2007.

[8] G. Golub and C. Van Loan, *Matrix Computations*, 3rd ed. Baltimore, MD: Johns Hopkins Univ. Press, 1996.